Mon. Not. R. astr. Soc. (1991) **251**, 128–136

Dynamical effects of the cosmological constant

Ofer Lahav,[1] Per B. Lilje,[2] Joel R. Primack[3] and Martin J. Rees[1]

[1] *Institute of Astronomy, Madingley Road, Cambridge CB3 0HA*
[2] *NORDITA, Blegdamsvej 17, DK-2100 Copenhagen Ø, Denmark*
[3] *Physics Department, University of California, Santa Cruz, CA 95064, USA*

Accepted 1991 February 21. Received 1991 February 21; in original form 1991 January 21

SUMMARY

The possibility of measuring the density parameter Ω_0 and the cosmological constant $\lambda_0 \equiv \Lambda/(3H_0^2)$ using dynamical tests is explored in linear and non-linear theory. In linear theory we find that the rate of growth of the perturbations at the present epoch is approximated by $f(z=0) \approx \Omega_0^{0.6} + \frac{1}{70}\lambda_0(1+\frac{1}{2}\Omega_0)$. Therefore, dynamical tests such as infall around clusters and dipoles at the present epoch do not distinguish well between universes with and without a cosmological constant. At higher redshifts, the perturbations also depend mainly on the matter density at a particular epoch, $f(z) \approx \Omega^{0.6}(z)$, which has a strong dependence on λ_0 at $z \approx 0.5$–2.0. Therefore, information on both parameters can be obtained by looking at clustering at different redshifts. In practice, however, the other observables also depend on the cosmology, and in some cases conspire to give a weak dependence on λ_0. By using the non-linear spherical infall model for a family of Cold Dark Matter (CDM) power-spectra we also find that dynamics at $z=0$ does not tell much about λ_0. At higher redshifts there is unfortunately another conspiracy between conventional observables, which hides information about λ_0. The final radius of a virialized cluster (relative to the turn-around radius) is approximated by $R_f/R_{ta} \approx (1-\eta/2)/(2-\eta/2)$, where η is the ratio of Λ to the density at turn-around. Therefore a repulsive Λ gives a smaller final radius than a vanishing Λ.

1 INTRODUCTION

The Cosmological constant Λ has had a chequered past. Einstein introduced a positive Λ (universal spatial repulsion) to counterbalance the gravitational attraction of matter in order to get a static universe (Einstein 1917; Kerszberg 1989). Eddington–Lemaître cosmologies, which have large spatial volume interval at some intermediate redshift range (the coasting period), were invoked to explain the abundance of quasars at $z \sim 2$–3 (e.g. Petrosian, Salpeter & Szekeres 1967). Although these previous appeals to Λ are now thought to be misguided, Λ is becoming popular in cosmology again in order to help resolve a number of problems.

(i) There is a conflict between globular cluster estimates of the age of the Universe (Sandage & Cacciari 1990) and the age estimated for $\Lambda = 0$ and a large value of the Hubble parameter $H_0 \approx 75$ km s^{-1} Mpc^{-1}, that seems increasingly to be favoured by observations (see, e.g. Fukugita & Hogan 1990).

(ii) Inflation implies vanishing curvature $K=0$ (e.g. Peebles 1984; Turner, Steigman & Krauss 1984; Linde 1990), i.e. $\Omega_0 + \lambda_0 = 1$ where $\lambda_0 \equiv \Lambda/3H_0^2$, so if $\Omega_0 \approx 0.2$, as suggested by some observations, then $\lambda_0 \approx 0.8$.

(iii) Number counts of galaxies at high redshifts (e.g. Tyson 1988) are incompatible with $\Omega = 1$ without a possibly unrealistic degree of merging. By increasing the spatial volume interval at high redshift, a lower Ω and/or a positive Λ may avoid this problem (Cowie & Lilly, private communication). Indeed Fukugita *et al.* (1990a) suggest that with no merging, $\Omega_0 = 0.1$ and $\lambda_0 = 0.9$ give the best fit to existing data.

(iv) Finally, the 'standard' Cold Dark Matter (CDM) model (Blumenthal *et al.* 1984; Davis *et al.* 1985) with $\Omega = 1$, Harrison–Zeldovich primordial fluctuations spectrum and a simple prescription for biasing, apparently predicts substantially less large-scale structure than observations indicate (Efstathiou, Sutherland & Maddox 1990). A lower $\Omega_0 \approx 0.2$ gives more large-scale structure since with later matter dominance the bend in the CDM fluctuation spectrum is shifted to larger scales (e.g. Blumenthal, Dekel & Primack 1988; Holtzman 1989), but this is incompatible with observational limits on cosmic background radiation fluctuations for $\Lambda = 0$, but not incompatible if $\lambda_0 = 1 - \Omega_0$ (Vittorio & Silk 1984; Kofman & Starobinsky 1985; Bond *et al.* 1990; Sugiyama, Gouda & Sasaki 1990). (There are of course other ways to modify CDM to increase the amount of large-scale power.)

Observationally, $|\lambda_0| \lesssim 1$ (see below), or $|\Lambda| \lesssim \rho_{\rm crit} = 3.64 \times 10^{-123} h^{-2} M_{\rm Pl}^4$, where the Planck mass $M_{\rm Pl} = G_N^{-1/2} = 1.22 \times 10^{19}$ GeV. From the viewpoint of fundamental physics (Weinberg 1989), the 'natural' values for Λ are either 0 or $\sim M^4$, where $M \sim M_{\rm Pl}$, or perhaps M is of the same order as a spontaneous-symmetry-breaking scale $M_{\rm GUT} \sim 10^{15}$ GeV or $M_{\rm W} \sim 10^2$ GeV. Since all of these mass scales are so much larger than the upper bound on $\Lambda^{1/4}$, it is tempting to try to find a physical reason why $\Lambda = 0$. For a time, it looked like quantum wormholes might provide such a mechanism (Coleman 1988; Banks 1988). However, it now appears that the situation is much more complicated than these first papers foresaw (see, e.g. Klebanov 1990), although it is still possible that a convincing argument for $\Lambda = 0$ can eventually be constructed along these lines. If this does not succeed, it will remain possible that we will some day understand why Λ is small but non-zero (for some hints along these lines, see, e.g. Rabinovici, Saering & Bardeen 1987; Veneziano 1989). For general reviews on Λ, see Stabell & Refsdal (1966), Rindler (1977), Felten & Isaacman (1986), Peebles (1988) and Weinberg (1989).

Maybe there is a reason why $\Omega_{\rm baryon,0}$, $\Omega_{\rm DM,0}$, and λ_0 are all of order unity. Our attitude is that we should try to put limits on λ_0 and Ω_0 regardless of theoretical prejudice, and thus consider curvature $K \neq 0$ models also, and that it is always useful to develop new ways of analysing the available data. In particular, we attempt to see what can be learned about Λ from the recent redshift and peculiar velocity surveys.

Of course, all known methods to measure the fundamental cosmological parameters have difficulties. Evolutionary and other poorly understood corrections are important for all geometrical methods, and the possibility that visible objects may be poor tracers of the underlying mass distribution ('biasing') is a problem with dynamical methods.

Although it is possible to measure the cosmological density parameter Ω_0 both geometrically (e.g. by number counts versus redshift) and dynamically (e.g. by infall), for the cosmological constant λ_0 only geometrical tests have usually been considered. Indeed, Peebles (1984) showed, for the inflationary case $K = 0$, that the infall peculiar velocity is essentially independent of λ_0. However, while this is true at the present epoch, for redshift z in the range 0.5–2.0 the rate of growth of perturbations is actually quite sensitive to λ_0 but rather insensitive to Ω_0. But we show that the observable parameters of clusters conspire to give a rather small dependence on λ_0.

This paper is organized as follows. In Section 2 we explore the $(\Omega_0 - \lambda_0)$ phase-space given fundamental observations. In Section 3 we discuss dynamical tests in linear theory, and in Section 4 non-linear tests like density and velocity profiles around clusters and virialization. In Section 5 we consider possible observations and in Section 6 we discuss the results.

2 FUNDAMENTAL LIMITS ON THE COSMOLOGICAL CONSTANT

Before considering the dynamical tests, we review here the limits on Λ from basic considerations. The 'energy' and 'motion' Friedmann equations for the scale factor $a = (1+z)^{-1}$ in a Universe dominated by non-relativistic matter and with zero pressure are (e.g. Peebles 1980)

$$\frac{\dot{a}^2}{a^2} = \frac{8\pi}{3} G\rho_{\rm b} + \frac{\Lambda}{3} - \frac{K}{a^2}, \tag{1a}$$

$$\ddot{a} = -\frac{4\pi}{3} G\rho_{\rm b} a + \frac{\Lambda}{3} a, \tag{1b}$$

where the derivatives are with respect to time, $\rho_{\rm b}$ is the background density (which varies like a^{-3} in a matter-dominated universe), Λ is the cosmological constant, and K is the curvature (which may be negative). The curvature can be specified in terms of present-day parameters:

$$K = H_0^2(\Omega_0 - 1) + \frac{\Lambda}{3}, \tag{2}$$

where $H_0 = (\dot{a}/a)_0$ is the Hubble constant and $\Omega_0 = \rho_0 8\pi G/(3H_0^2)$ is the density parameter. We take the value of the scale factor at the present to be $a_0 = 1$. It is also convenient to express the cosmological constant as $\lambda_0 = \Lambda/(3H_0^2)$. We explore now the $(\lambda_0 - \Omega_0)$ parameter space, given fundamental constraints such as the age of the Universe and its origin in a Big Bang. The condition for no Big Bang origin is given by analytic expressions in Felten & Isaacman (1986). This regime is shown at the bottom right corner of Fig. 1. A large λ_0 may give a 'bounce' model, which started with a large-scale factor, reached a minimum value a_*, and then expanded. A stringent constraint on bounce models comes from the fact that quasars are observed at high redshifts. The conditions for a bounce model [on both $\dot{a}$ and $\ddot{a}$ in equations (1a and b), so λ_0 is eliminated] give an upper limit on Ω_0 for a given max-

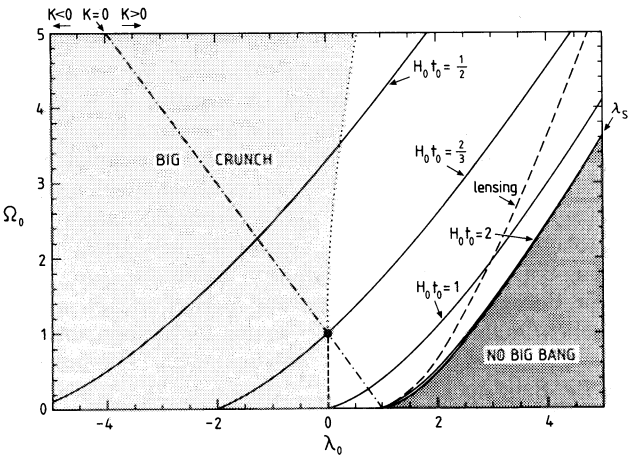

Figure 1. The phase-space of the density parameter Ω_0 and the cosmological constant $\lambda_0 \equiv \Lambda/(3H_0^2)$ with various fundamental constraints. The dashed-dotted line indicates an inflationary (i.e. flat) universe. Note that some open models will have a Big Crunch, while some closed models will expand forever. The solid lines show 4 values for the age of the universe $H_0 t_0$, and the dashed line is the constraint of Gott *et al.* (1989) from a normally lensed quasar at $z = 3.27$. The boundary (λ_s) of the shaded 'No Big Bang' region corresponds to a coasting phase in the past, while the boundary of the 'Big Crunch' (for $\Omega_0 > 1$) region corresponds to a coasting phase in the future. We see that the permitted range in the $(\lambda_0 - \Omega_0)$ phase-space is fairly small, but allows values different from the popular point $(\Omega_0 = 1, \lambda_0 = 0)$.

imal observed redshift $z_* = a_*^{-1} - 1$ (e.g. Felten & Isaacman 1986; Peebles 1988; Börner & Ehlers 1988): $\Omega_0 \leq 2 z_*^{-2}(z_* + 3)^{-1}$. The most distant known quasar is at $z = 4.73$ (Schneider, Schmidt & Gunn 1989), so if $\Omega_0 > 0.01$ (as indicated from several observational tests), bounce models are most probably ruled out. We also show on the left the region of parameter space corresponding to a Big Crunch ending (which of course is not a constraint as yet!).

The dashed-dotted line is for $K = 0$ or $\Omega_0 + \lambda_0 = 1$, i.e. a flat universe as favoured by inflation. The regime to the right of this line corresponds to $K > 0$ (closed Universe), and to the left to $K < 0$ (open Universe). Note that some open models will have a Big Crunch, while some closed models will expand forever.

The age constraint comes from measurements of the Hubble constant (observed to be $50 \leq H_0 \leq 100$ km s^{-1} Mpc^{-1}, and the age of globular clusters (estimated to be in the range $13 \leq t_0 \leq 17$ Gyr, e.g. Sandage & Cacciari 1990). Therefore we get observationally the range $0.7 \leq H_0 t_0 \leq 1.7$. From equation (1) we can get the age as a function of Ω_0 and λ_0:

$$H_0 t_0 = \int_0^1 \frac{a^{1/2}\, da}{[\lambda_0 a^3 + (1 - \Omega_0 - \lambda_0) a + \Omega_0]^{1/2}}. \tag{3}$$

This relation is shown for fixed values of $H_0 t_0$ in Fig. 1.

We also show a new gravitational lensing constraint (Gott, Park & Lee 1989). In cosmologies with large positive Λ, the redshift of the antipodes is relatively small. A gravitationally lensed QSO lying at a larger redshift than the antipodal redshift will typically have only one image. The existence of an apparently normally lensed QSO at $z = 3.27$ implies that the antipodal redshift is greater than that, which translates into the dashed curve in Fig. 1. An 'anthropic' upper bound on Λ (which is quite large) can be determined by the condition that Λ has to be small enough to allow the formation of condensations by gravity (Weinberg 1987, 1989). We see that the permitted range is fairly narrow. A negative λ_0 is mostly eliminated by the age constraint (and also has a less obvious physical interpretation), and the theoretically popular point on this plane, ($\Omega_0 = 1$, $\lambda_0 = 0$), is only consistent with a young Universe ($H_0 t_0 = \frac{2}{3}$). While $H_0 t_0$ grows arbitrarily large as one approaches the 'no Big Bang' region, the new gravitational lensing constraint limits the extent to which one can appeal to an Eddington–Lemaître coasting period to get an old universe. On the other hand, we see that for example the case ($\Omega_0 = 0.1$, $\lambda_0 = 0.9$), which is consistent with both inflation and Big Bang nucleosynthesis constraints on $\Omega_{\rm baryon}$ (Olive *et al.* 1990), looks fine.

3 DYNAMICS IN LINEAR THEORY

The linearized equation for the growth of perturbations is given by (e.g. Peebles 1980):

$$\frac{\partial^2 \delta}{\partial t^2} + 2 \frac{\dot{a}}{a} \frac{\partial \delta}{\partial t} = 4\pi G \rho_{\rm b} \delta, \tag{4}$$

where $\delta \equiv \delta\rho/\rho$.

Health (1977) showed that the growing mode as a function of the scale factor a [which obeys equation (1)] is

$$\delta \propto H_0^{-2} X^{1/2} a^{-1} \int_0^a X^{-3/2}\, da, \tag{5}$$

where $X \equiv 1 + \Omega_0(a^{-1} - 1) + \lambda_0(a^2 - 1)$.

In linear theory the peculiar velocity $\boldsymbol{v}_{\rm pec}$ is related to the peculiar acceleration $\boldsymbol{g}$ by (Peebles 1980, Section 14)

$$\boldsymbol{v}_{\rm pec} = \frac{2f\boldsymbol{g}}{3H\Omega}, \tag{6}$$

where

$$f \equiv \frac{d \ln \delta}{d \ln a}. \tag{7}$$

This relation is basically derived from the linearized continuity equation, with the assumption that the growth rate of structure is independent of position. Another variant of this equation is the radial infall velocity around a spherical perturbation of radius R and with interior average overdensity $\langle\delta\rangle_R$,

$$\frac{v_{\rm pec}}{HR} = \frac{1}{3} f \langle\delta\rangle_R. \tag{8}$$

These expressions, evaluated at the present epoch ($z = 0$) have been used to compute the value of Ω_0 (assuming zero cosmological constant) from the Virgo infall and *IRAS* and optical dipoles (e.g. Yahil 1985; Yahil, Strauss & Davis 1989; Lynden-Bell, Lahav & Burstein 1989), and also from the local peculiar velocity field compared to the distribution of *IRAS* galaxies (see below).

Here we generalize the calculation for any values of Ω_0 and λ_0 at any redshift z. By differentiating equation (5) with respect to a and using equation (7) we get

$$f(\Omega_0, \lambda_0, z) = X^{-1}\left[\lambda_0 (1+z)^{-2} - \frac{\Omega_0}{2}(1+z)\right] - 1 + (1+z)^{-1} X^{-3/2} \Big/ \int_0^{(1+z)^{-1}} X^{-3/2}\, da, \tag{9}$$

where $X \equiv 1 + \Omega_0 z + \lambda_0[(1+z)^{-2} - 1]$. This expression yields, in special cases, well-known results. For ($\Omega_0 = 1$, $\lambda_0 = 0$) one gets $f = 1$ for all z, since $\delta \propto a$. For ($\lambda_0 = 0, z = 0$) one can write the solution in terms of a Hypergeometric function, $f = -\Omega_0/2 - 1 + \frac{5}{2}\Omega_0^{3/2}/F(\frac{3}{2}, \frac{5}{2}, \frac{7}{2}, 1 - \Omega_0^{-1})$. Convenient approximations are $f \approx \Omega_0^{0.6}$ (Peebles 1980) or $f \approx \Omega_0^{4/7}$ (Lightman & Schechter 1990). We find the following approximation for $f(\Omega_0, \lambda_0)$ at $z = 0$ in the range $-5 \leq \lambda_0 \leq 5$, $0.03 \leq \Omega_0 \leq 2$ (in the allowed zones):

$$f(z=0) \approx \Omega_0^{0.6} + \frac{1}{70}\lambda_0\left(1 + \frac{1}{2}\Omega_0\right). \tag{10}$$

The mean error in this approximation is 2 per cent (with a maximum error of 33 per cent in the low-Ω_0 case). A different approximation is given by Martel (1991b). Equation (10) generalizes the result of Peebles (1984), who only considered the case $\Omega_0 + \lambda_0 = 1$. We see that at $z = 0$, f is almost entirely determined by Ω_0, with a very weak dependence on λ_0. Since the dynamics at $z = 0$ depends mainly on the present matter

density, it suggests that f depends on $\Omega(z)$ at any epoch, Indeed we find that $f(z)$ is well approximated for any z, λ_0 and Ω_0 by

$$f(z)\approx\Omega^{0.6}, \tag{11a}$$

where

$$\Omega(z,\Omega_0,\lambda_0)=\Omega_0(H/H_0)^{-2}(1+z)^3, \tag{11b}$$

and

$$(H/H_0)^2=\Omega_0(1+z)^3-(\Omega_0+\lambda_0-1)(1+z)^2+\lambda_0. \tag{11c}$$

For a flat universe ($K=0$) an even better approxmation is provided by analogy with equation (10), $f(z)\approx\Omega^{0.6}+\frac{1}{70}[1-\frac{1}{2}\Omega(1+\Omega)]$.

Table 1 gives the exact numerical value of f for various values of Ω_0, λ_0 and z. Fig. 2 shows the evolution of f with redshift for different pairs of (Ω_0,λ_0). We see that at higher z the value of f is more sensitive to λ_0. In particular in the range $z\approx0.5$–2.0 it is possible to discriminate between universes with different cosmological parameters. The high peak for the $K>0$ cases is due to a 'coasting phase' in which the scale factor changes very slowly while the perturbations grow exponentially. This is related to the proposal (Petrosian, Salpeter & Szekeres 1967; Shklovsky 1967; Rowan-Robinson 1968) that the 'coasting phase' could give rise to the high abundance of quasars at $z\approx2$. A 'coasting phase' is a very efficient way of producing large-scale structure at recent epochs, but it corresponds to non-inflationary models (it is worth mentioning, however, that some special inflationary models allow a non-zero curvature, e.g. Steinhardt 1990). Fig. 3 shows lines of fixed $f=1$ in the $(\Omega_0-\lambda_0)$ plane. Again we see that f is changing from being Ω_0-dominated at $z=0$ to λ_0-dominated at higher z.

Table 1. Growth factor f for certain values of Ω_0, λ_0, and z.

	$\Omega_0=0.2$			$\Omega_0=1.0$		
λ_0	-1	0.0	0.8	-1.0	0.5	1.0
z						
0.00	0.362	0.383	0.407	0.976	1.014	1.029
0.25	0.345	0.427	0.539	0.854	1.100	1.231
0.50	0.354	0.464	0.650	0.828	1.128	1.311
0.75	0.369	0.496	0.736	0.825	1.132	1.324
1.00	0.386	0.524	0.801	0.830	1.127	1.309
1.50	0.420	0.571	0.883	0.845	1.111	1.263
2.00	0.452	0.610	0.927	0.861	1.096	1.222
3.00	0.506	0.668	0.967	0.886	1.074	1.164
4.00	0.551	0.711	0.983	0.904	1.059	1.129
5.00	0.588	0.744	0.990	0.917	1.049	1.106

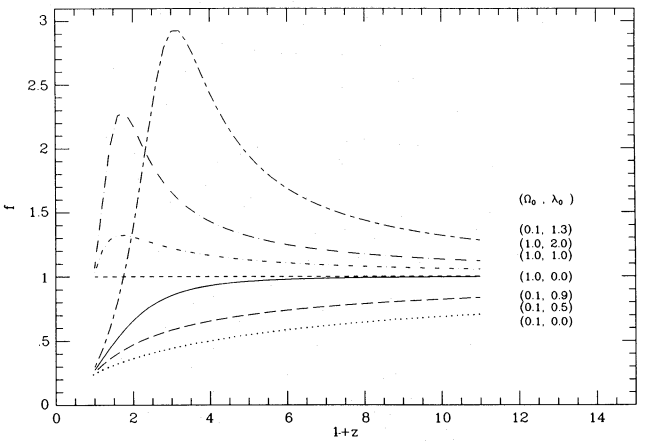

Figure 2. The evolution of the growth factor of the perturbations $f\equiv d(\ln\delta)/d(\ln a)$ with redshift for different pairs of (Ω_0,λ_0). Note that for a given Ω_0 the growth factor depends very weakly on λ_0 at $z=0$, but is much more sensitive to λ_0 at higher redshifts.

Another interpretation of the dynamical test of equation (8) crucially depends on how the observables are actually deduced. For example, since $f\approx\Omega^{0.6}$, the product $fH\approx\Omega_0^{0.6}H_0(1+z)^{1.8}(H/H_0)^{-0.2}$ depends only weakly on λ_0. In this case it is only possible to have some dependence on λ_0 by measuring the peculiar velocity and the over-density (say in a model-independent way) and estimating the metric radius $R\sim v_{\rm pec}/\langle\delta\rangle_R$, and then using the angle-redshift relation to learn about λ.

The angular radius θ of an object with metric radius R at a cosmological distance can be found directly from the Robertson–Walker metric and the Friedmann equations. It depends on the integral

$$\omega=\int_{(1+z)^{-1}}^{1}\frac{dx}{x\sqrt{\Omega_0(x^{-1}-1)+1-\lambda_0(1-x^2)}}. \tag{12}$$

For $\lambda_0=0$ this can be solved analytically, but generally it must be solved numerically. For the curved cases the solutions depend on the curvature parameter (*cf.* equation 2) $k=\sqrt{|K|}/H_0=\sqrt{|\Omega_0+\lambda_0-1|}$. The solution for the three cases are as follows,

$$\Omega_0+\lambda_0=1:\qquad\theta=\frac{H_0R(1+z)}{c\omega}; \tag{13a}$$

$$\Omega_0+\lambda_0>1:\qquad\theta=\frac{H_0R(1+z)\,k}{c\sin(k\omega)}; \tag{13b}$$

$$\Omega_0+\lambda_0<1:\qquad\theta=\frac{H_0R(1+z)\,k}{c\sinh(k\omega)}. \tag{13c}$$

4 NON-LINEAR SPHERICAL MODELS

In the previous section we found that dynamical tests for λ_0 in linear theory are only useful at high redshifts. In this section we explore the possibility of using *non-linear* theory at $z=0$ and at higher redshifts. In particular we look at density and velocity profiles around clusters in the mildly non-linear regime, and at the final state of collapse (virialization).

4.1 Spherical infall

A simple extension to the non-linear regime can be made by considering the non-linear spherical model. The evolution of spherical shells has been discussed extensively for the $\lambda_0=0$ case by Gunn & Gott (1972) and others, for the $\Omega_0+\lambda_0=1$ case by Peebles (1984) and Weinberg (1987), and in relation with voids (for any λ_0) by Martel & Wasserman (1990). Martel (1991b) discussed the evolution of particular spherical surfaces. N-body simulations with Λ were carried out by Davis *et al.* (1985), Gramann (1990), and Martel (1991a), showing that Λ has little effect on the dynamics at the present epoch.

In the case of a universe with Λ, the Tolman–Bondi equation for the energy per unit mass for a shell enclosing mass m is:

$$\varepsilon(m)=\frac{1}{2}\dot{R}^2-\frac{Gm}{R}-\frac{1}{6}\Lambda R^2, \tag{14}$$

so essentially the potential energy is modified by the Λ-term, which behaves (for negative Λ) like a harmonic oscillator.

Here we discuss infall for initial conditions of a family of Cold Dark Matter models, which has been discussed in detail in recent years. For $\Omega_0 h=0.2$ the CDM power spectrum provides a phenomenological fit to the APM angular correlation function (Efstathiou *et al.* 1990) on the scales which are relevant to the infall problem ($\sim 10\ h^{-1}$ Mpc, where $H_0=100\ h$ km s^{-1} Mpc^{-1}).

We have generalized the procedures which Lilje & Lahav (1991, hereafter LL) used to estimate the average behaviour of the density and velocity fields around clusters of galaxies. LL used the theory of the statistics of peaks in Gaussian random fields and linear gravitational-instability theory to compute the average radial density and peculiar velocity profiles at an early initial epoch around what would become clusters of galaxies. They then used the spherical infall model to evolve the initial profiles to the present epoch.

Here we use the same method to set up the initial conditions for a protosupercluster at $z=1000$ [equations (3.1), (3.6), (4.3) and (4.5) of LL], with a few changes. The primordial power spectrum does not depend on Λ (since at early epochs the Λ-term is very small compared with the other terms), but a non-zero Λ allows a zero-curvature (inflationary) universe with $\Omega_0\neq 1$.

We use the fits to the CDM power spectrum given by Bardeen *et al.* (1986) for $\Omega_0\neq 1$ with a Gaussian filter of radius $3\ h^{-1}$ Mpc. The amplitude of the power spectrum is determined by the requirement that the present rms fluctuations within a spherical volume with $8\ h^{-1}$ Mpc radius equals b^{-1} (where b is the 'biasing' parameter).

We define as clusters all peaks in the filtered density field, which are higher than a sharp threshold. This threshold is fixed by the requirement that the present number density of clusters is $10^{-5}(h^{-1}\ \mathrm{Mpc})^{-3}$. The initial amplitude of the fluctuations [$\delta_i(r)$ and $\Delta_i(r)$] are determined from equation (5), while the initial velocity fluctuation is given by equation (9), so that

$$a_i=-\frac{2}{3}\,f(\Omega_0,\lambda_0,z_i)\,\Delta_i. \tag{15}$$

We also need the initial Hubble constant H_i (equation 11b) and the initial density parameter Ω_i (equation 11c), although when z_i is as high as 1000, Ω_i and $f(\Omega_0,\lambda_0,z_i)$ will be indistinguishable from unity.

Because of the cosmological constant, we cannot use the analytic solution of the equation of motion for a spherical shell. Instead it has to be integrated numerically. The initial radius of a shell in comoving coordinates is r_i, and the physical radius at time t is

$$R(t)=A(t,r_i)(1+z_i)^{-1}r_i, \tag{16}$$

where A is the scale-factor of the shell. When we introduce the time parameter $\tau=H_i t$, the equation of motion is

$$\frac{d^2A}{d\tau^2}=-\frac{1}{2}(1+\Delta_{ci})A^{-2}+\lambda_i A, \tag{17}$$

where

$$\lambda_i=\left(\frac{H_0}{H_i}\right)^2\lambda_0, \tag{18}$$

and where Δ_{ci} is the initial density contrast relative to the critical density. The initial conditions are $A(\tau_i)=1$ and $dA/d\tau(\tau_i)=(1+\alpha_i)^{1/2}$. To be able to integrate this equation more accurately, we write it in terms of the difference from a shell comoving with an unperturbed $\Omega_0=1$, $\lambda_0=0$ universe, so that

$$A(\tau)=\tilde{A}(\tau)+A_1(\tau), \tag{19}$$

where

$$\tilde{A}(\tau)=\left(\frac{3}{2}\tau\right)^{2/3}. \tag{20}$$

The equation for A_1 is integrated numerically from $\tau=H_i t_i$ to $\tau=H_i t_f$. We stop the integration if A reaches zero. That means that the shell has collapsed, and we place it in the cluster core. The age of the Universe at the initial and final redshifts is found equivalently to equation (3), but with the upper integration boundary replaced with $(1+z)^{-1}$. At the final time, the radial velocity of the shell is

$$v(r_i,t_f)=H_i\frac{dA}{d\tau}(\tau_f)(1+z_i)^{-1}r_i, \tag{21}$$

so that the peculiar infall velocity is

$$v_{\mathrm{infall}}=H_f R(r_i,t_f)-v(r_i,t_f). \tag{22}$$

The density perturbation at distance R at $t=t_f$ is, from the continuity equation,

$$\delta(R)=\frac{(1+\bar{\delta}_i)(1+z_i)^3}{A^3(1+z_f)^3\left(1+r_i\dfrac{A'}{A}\right)}-1, \tag{23}$$

where $A'=dA(r_i)/dr_i$ is differentiated numerically.

Figs 4 and 5 show the average density and velocity profiles around clusters at $z=0$ and $z=0.5$ for four different CDM models. The first model (solid line) is the 'standard' biased CDM model with $\Omega_0=1$, $\lambda_0=0$, $h=0.5$ and $b=2$. The other three models are unbiased low-density CDM models with $\Omega_0=0.2$, $h=1$, and $b=1$. One is open with $\lambda_0=0$ (short dashed line), the second is flat ('inflationary') with $\lambda_0=0.8$ (long dashed line), and the third is 'non-inflationary' with $\lambda_0=1.3$ (dash-dotted line). The open model is probably ruled out from the microwave background constraints, but we use it here to investigate the effect of varying λ_0 while holding all other parameters fixed.

We see that the change in the initial power spectrum due to a change in Ω_0 gives a strong imprint on the average density profile ($b\delta$ which is the cluster–galaxy correlation function ξ_{cg}). However, changing λ_0 while keeping Ω_0 fixed has almost no effect (all three lines lie on top of each other). That is because the power spectrum (which is independent of λ_0) is normalized at the present epoch, and Λ could only

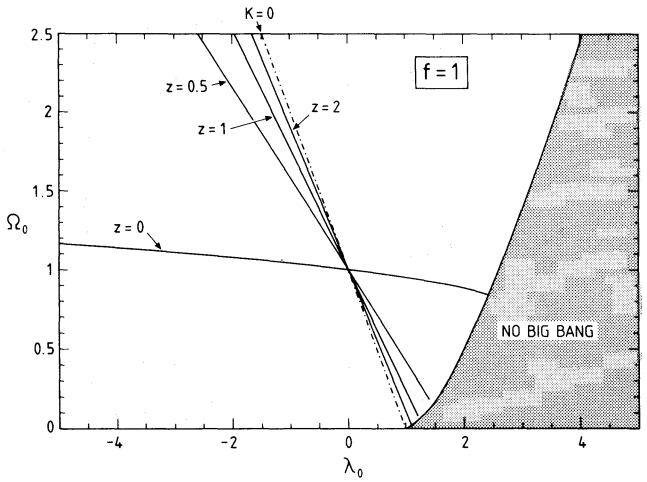

Figure 3. Lines of fixed $f=1$ for different redshifts in the $(\Omega_0-\lambda_0)$ plane. The growth factor f is changing from being Ω_0-dominated at $z=0$ to λ_0-dominated at higher z.

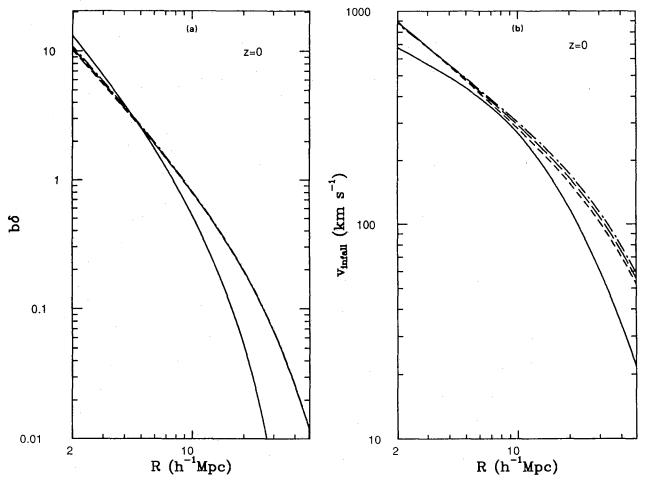

Figure 4. The average density (4a, left panel) and velocity (4b, right panel) profiles as a function of radius around clusters at $z=0$, for different CDM models: the 'standard' biased CDM model with $\Omega_0=1$, $\lambda_0=0$, $h=0.5$ and $b=2$ (solid line), and three CDM models with $\Omega_0=0.2$, $h=1$, $b=1$, and with $\lambda_0=0$ (short-dashed line), $\lambda_0=0.8$ (long-dashed line), and $\lambda_0=1.3$ (dash-dotted line). We see that changing λ_0 while keeping Ω_0 fixed has almost no effect (all three lines lie nearly on top of each other).

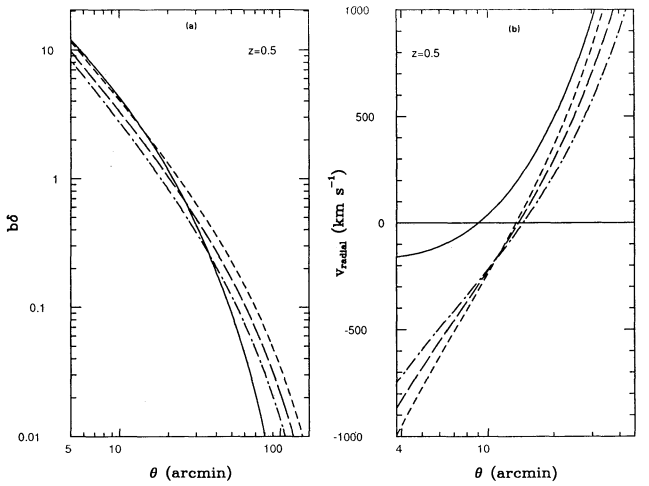

Figure 5. The average density (5a, left panel) and velocity (15b, right panel) profiles as a function of angular separation around clusters at $z=0.5$. The four CDM models are as in Fig. 4. Unfortunately, the various cosmological factors involved conspire to tell little about λ_0.

have changed the density profile by its effect on the non-linear motion of shells. However, at small separations where the velocity field is non-linear, the effect of Λ is small. (It is possible to see a slight difference in the lines at small distances, but they overlap completely on larger scales.) For the velocity field we again see the marked difference between the $\Omega_0=1$ model and the $\Omega_0=0.2$ models, but we see that as for linear theory, the change made by only varying λ_0 is very small. We see that at the present epoch the density and velocity fields around clusters of galaxies cannot be used to distinguish between models with different λ_0 and all other parameters fixed.

To define which peaks in the density field would be seen as high redshift clusters is quite model dependent (e.g. Evrard 1989). To test the effects of a cosmological constant on density and velocity fields we here assume that the clusters seen at $z=0.5$ have the same peak height in units of the rms density fluctuations as clusters at the present epoch. This might be an underestimate since the rms fluctuations were smaller, but by how much is model dependent. At $z=0.5$ the average density as a function of metric distance from the cluster centre shows the same picture as at the present epoch. The 'standard' model has a somewhat lower amplitude compared to $z=0$ because the growth factor from $z=0.5$ to the present is larger. The models with $\Omega_0=0.2$ are still not very different. The linear growth factors for those are rather similar (linear perturbations have grown by 19 per cent, 24 per cent and 30 per cent from $z=0.5$ to the present for the models with $\lambda_0=0$, 0.8 and 1.3 respectively), and non-linear evolution has not changed the picture significantly. However, metric separation is not an observable quantity at cosmological distances. In Fig. 5(a) we have plotted the average density field around a cluster as a function of angular separation, which probably would be the relevant observable quantity. The angular separation has been computed from equations (13). We see that now there is a difference between the different λ_0 curves. The use of this version of the angular distance–redshift test would be difficult however, due to the small size of the effect and the strong model dependence of the cluster–galaxy cross-correlation function.

Any measurement of velocity fields around high-redshift clusters would be extremely difficult. The least difficult observation we can think of is the distance from the cluster of the zero-velocity surface. This is seen as the endpoints of the caustics in plots of the positions of galaxies around clusters in redshift space (e.g. Regös & Geller 1989). In metric separation this distance varies by a factor of ~20 per cent between the models with $\Omega_0=0.2$. In Fig. 5(b) we plot radial velocity (cosmic expansion velocity minus the peculiar infall velocity) as function of angular separation. Unfortunately the angular size–redshift relation works in the opposite direction to the

effect on metric distance, and it conspires to put the zero-velocity surfaces at almost the same angular distance for all low-density models. It is worth mentioning that a universe with large positive Λ, in which the antipodal redshift is rather small, a cluster at redshift near the antipodal redshift will have an unusual angular size (*cf.* equation 13), so this provides another observational constraint on Λ. In linear theory (equations 8 and 22) the radial velocity is proportional to $H_f R$, and in the weakly non-linear regime this should also almost be the case. Therefore the value of H_f has no influence on the position of the zero-point, and the conspiracy here is not the same as the *fH* conspiracy of Section 3. It is rather caused by the combination of the slope of the density profile (close to R^{-2}), the angle–redshift relation, and the growth factor of perturbations, f. The different values of H_f causes different slopes in Fig. 5(b). We again see that the $\Omega_0 = 1$ model differs significantly from the $\Omega_0 = 0.2$ models. At high redshifts the conclusions are the same as at low redshifts: density and velocity fields around clusters of galaxies give strong constraints on the initial power spectrum, Ω_0 and b, but not independently on λ_0.

4.2 Virialization with Λ

In a Universe with $\Lambda = 0$ the well-known result is that the 'final' effective radius of a collapsing cloud is half its turn-around radius. The virial theorem relates the kinetic energy T to a potential energy of the form $U \propto R^n$ by (e.g. Landau & Lifshitz 1960)

$$T = \frac{n}{2} U, \tag{24}$$

where the energies of the system are averaged over time.

We assume a uniform sphere with a turn-around outer radius R_{ta}. The total mass in terms of the turn-around density is $M = (4\pi/3)\rho_{ta} R_{ta}^3$. By integrating the terms in equation (14) over a sphere we get the potential energies at turn-around due to gravity and Λ, $U_{G,ta} = -\frac{3}{5} GM^2/R_{ta}$ and $U_{\Lambda,ta} = -\frac{1}{10}\Lambda M R_{ta}^2$. Using the virial theorem we can write for the final state

$$T_f = -\frac{1}{2} U_{G,f} + U_{\Lambda,f}. \tag{25}$$

Since the energy is conserved, we can write $E = T_f + U_{G,f} + U_{\Lambda,f} = U_{G,ta} + U_{\Lambda,ta}$, and using equation (25) one gets $\frac{1}{2} U_{G,f} + 2U_{\Lambda,f} = U_{G,ta} + U_{\Lambda,ta}$. We now define the effective final radius of the system (in analogy to the initial energies and assuming that the sphere remained uniform) by $U_{G,f} = -\frac{3}{5} GM^2/R_f$ and $U_{\Lambda,f} = -\frac{1}{10}\Lambda M R_f^2$. This leads to the following cubic equation for the radio R_f/R_{ta}:

$$2\eta (R_f/R_{ta})^3 - (2+\eta)(R_f/R_{ta}) + 1 = 0, \tag{26}$$

where η specifies the strength of Λ relative to the density at turn-around.

$$\eta \equiv \frac{\Lambda}{4\pi G \rho_{ta}} = \frac{\Lambda R_{ta}^3}{3GM} \approx 0.06 \left(\frac{\lambda_0}{M_{15}}\right)\left(\frac{R_{ta}}{3h^{-1}\,\mathrm{Mpc}}\right)^3, \tag{27}$$

where M_{15} is the mass in units of $10^{15}\,M_\odot$ (a typical mass for a cluster). The condition for a shell to turn around is $\eta < 1$. ($\eta = 1$ is in fact analogous to the condition for the Einstein's static Universe.) The minimal possible ratio is $R_f/R_{ta} = 0.366$. An approximated solution (by expanding $R_f/R_{ta} = \frac{1}{2} + \varepsilon$ for small ε) to equation (26) is

$$\frac{R_f}{R_{ta}} \approx \frac{(1-\eta/2)}{(2-\eta/2)}. \tag{28}$$

Clearly, for $\lambda_0 = 0$ we recover the well-known result $R_f/R_{ta} = \frac{1}{2}$. Fig. 6 shows the exact solution to equation (26) (for $\eta > 0$ the cubic equation has two real roots, one of them corresponds to expanding shells) and the approximation (equation 28). We see that for a *repulsive* (positive) Λ the final radius is *smaller* compared with a zero-Λ case. The reason is that the shells have to fall further in order to acquire a velocity which will bring the system to an equilibrium. The reverse is true for negative Λ. With realistic values for λ_0 and the turn-around density, the effect is rather small. The effect is more important at late epochs, when the turn-around density is getting smaller.

5 RELEVANT OBSERVATIONS

At $z = 0$ there are several independent estimates for f. Both the Virgocentric infall model (e.g. Yahil 1985) and the optical dipole (Lynden-Bell *et al.* 1989) give, assuming no biasing, $f \approx 0.4$. The *IRAS* dipole (e.g. Strauss 1989) gives $f \approx 0.8$. A comparison of the *IRAS* density field (Yahil, Strauss & Davis 1990) to the matter density reconstructed from the peculiar velocity field (Dekel, Bertschinger & Faber 1990) yields (Yahil 1990; Bertschinger 1990) $f = 1.0 \pm 0.3$. Kaiser *et al.* (1991) found from the One-in-Six *IRAS* redshift survey $f = 0.9 \pm 0.2$. If we allow for biasing in the range $b \approx 1$–2 for optical galaxies and say $b \approx 1$–1.5 for *IRAS* galaxies, we find that the above observations give a fairly broad range, $f \approx 0.4$–1.2. This corresponds to $\Omega_0 \approx 0.2$–1.4, almost for any value of λ_0 (see equation 10).

As we emphasized earlier, a way to decouple the measurement of Ω_0 from λ_0 is by going to higher redshifts. There are

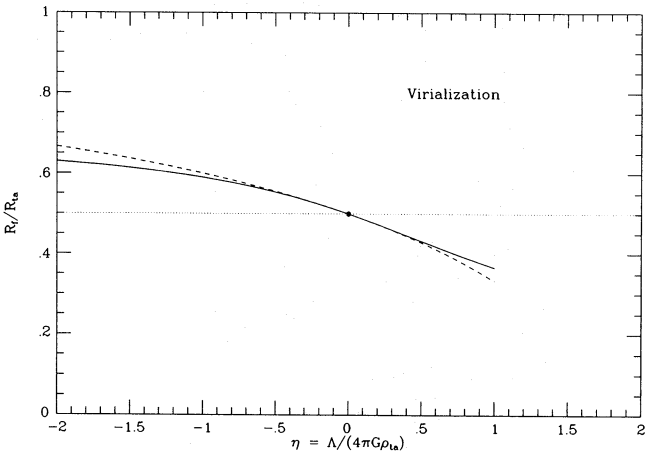

Figure 6. The ratio of the final to turn-around radius of a virialized cluster, as a function of η, the ratio of Λ to the density at turn-around. η cannot be larger than 1 in order for a collapse to occur. The solid line is the exact solution to equation (26) and the dashed line is the approximation (equation 28). A repulsive Λ gives a smaller final radius than a vanishing Λ.

measurements of clusters up to $z \approx 0.9$ (e.g. Gunn 1990). A good example is Abell 370 which is at $z = 0.374$, with velocity dispersion of 1350 km s^{-1} (Mellier *et al.* 1988). This cluster also has an impressive arc (Soucail *et al.* 1987) which, if attributed to gravitational lensing, allows us to estimate the true mass of the cluster, without the complications of biasing and evolution. Unfortunately, the velocity field has been mapped so far only in the cluster core ($\approx 0.4\ h^{-1}$ Mpc) where the overdensities are far larger than unity, and the cluster is non-spherical.

Another promising observation is the evolution of custering of quasars with redshift. For example, if the correlation function of quasars is almost constant in the redshift range $z = 0$–2 (Boyle 1991), then a scenario with $f(z) \approx 0$ is more favourable. We see from Table 1 and Fig. 2 that this may suggest a low present-day Ω_0 and a vanishing λ_0. Other possible probes of Λ are high-z superclusters of metal absorption line systems along the lines-of-sight to quasars (e.g. Jacobsen *et al.* 1986) and the Lyman-α clouds.

6 DISCUSSION

In this paper we have explored possible ways to learn about the cosmological parameters from dynamical tests. Our results are summarized as follows

(i) In linear theory the rate of growth of the perturbations at the present epoch is (equation 10)

$$f(z=0) \approx \Omega_0^{0.6} + \frac{1}{70}\lambda_0\left(1 + \frac{1}{2}\Omega_0\right),$$

so any deduction of λ_0 is nearly hopeless. This is essentially because Λ behaves like a uniform density field, hence the dynamics is only weakly affected by it. At higher redshifts the growth factor is (equation 11)

$$f(z) \approx \Omega^{0.6}(z),$$

which has a strong dependence on λ_0 at $z \approx 0.5$–2.0 (see Figs 2 and 3). However, the other quantities in the infall equation (equation 8) also depend on the cosmology, and in some cases conspire to give a weak dependence on λ_0.

(ii) By using the non-linear spherical infall model we find that dynamics at $z = 0$ also does not tell much about λ_0 (in agreement with N-body simulations, e.g. Martel 1991a). At higher redshifts there is unfortunately again a conspiracy between conventional observables which hides information about λ_0. However, a constraint on very large Λ is provided by the angular size–redshift relation.

(iii) The final radius of a virialized cluster (relative to the turn-around radius) is approximated by (equation 28):

$$\frac{R_f}{R_{ta}} \approx \frac{(1-\eta/2)}{(2-\eta/2)},$$

where η is the ratio of Λ to the density at turn-around. Therefore a repulsive Λ gives a smaller final radius, which cannot be smaller than about a third.

We conclude that present-day observations of density and velocity fields around clusters of galaxies cannot be used to distinguish between models with different λ_0 if all other parameters are fixed. However, they do give a good measure of the power spectra for galaxy density and mass density respectively, and therefore possibly of Ω_0. Since a low value of Ω_0 probably is incompatible with microwave background constraints without a cosmological constant, measurements of ξ_{cg} and velocity fields around clusters can give some constraints on λ_0 in an indirect way. Here we only considered spherical clusters. The effect of Λ on non-spherical ('pancake') collapse may exhibit a stronger signature. For example, for certain values of over-density and Λ, the 'pancake' will collapse in one axis, but will remain unbounded and eventually go into accelerating expansion along the other axes (Lemson, in preparation). High-redshift observations of clustering of galaxies and quasars are more promising, although their sensitivity depends on the combination of the observables. Another interesting aspect is the effect of Λ on the abundance of high-redshift objects (Lilje & Lahav, in preparation). Other possible high-z observations for Λ are gravitational lensing (e.g. Turner 1990, Fukugita, Futamase & Kasai 1990b) and the Sunyaev–Zeldovich effect (Silk & White 1978).

The present observations of the combination f/b (where b is the bias parameter) still allow many possibilities. If one prefers to adopt the 'paradigms' of inflation ($\Omega_0 + \lambda_0 = 1$), big bang nucleosynthesis (which suggests $\Omega_{baryon} < 0.1$) and some form of biasing (a constant one is clearly naive, but convenient for discussion), then two extreme possible pictures emerge. One is with a large amount of non-baryonic matter and zero cosmological constant. In this picture (represented for example by the Cold Dark Matter and Hot Dark Matter models) the galaxies are clustered stronger than the underlying mass distribution ($b > 1$). An alternative is to assume that all the matter in the Universe is baryonic, but to add a cosmological constant in order to save inflation (i.e. zero curvature), so $\Omega_0 = \Omega_{baryon}$ and $\Omega_0 + \lambda_0 = 1$. Such a model will suggest *anti-biasing* ($b < 1$), i.e. that galaxies are less clustered than the matter. One can still not rule out other possibilities of 'hybrid' scenarios (e.g. a universe with baryons, Cold Dark Matter and a cosmological constant) but they are less elegant.

ACKNOWLEDGMENTS

We thank J. Felten, D. Lynden-Bell, G. Soucail, and I. Wasserman for helpful discussions. This work was supported by a St Catharine's College Research Fellowship (OL) and NSF grant PHY-8800801 (JP). We wish to thank the Institute for Advanced Studies of the Hebrew University, where this work was started. We also thank the Institute of Astronomy in Cambridge and the Astrophysics Group at Oxford (JP) and NORDITA (OL) for their hospitality.

REFERENCES

Banks, T., 1988. *Nucl. Phys.*, **B309**, 493.
Bardeen, J. M., Bond, J. R., Kaiser, N. & Szalay, A. S., 1986. *Astrophys. J.*, **304**, 15.
Bertschinger, E., 1990. In: *Proc. of the Moriond Conference*, March 1990.
Blumenthal, G., Dekel, A. & Primack, J., 1988. *Astrophys. J.*, **326**, 539.
Blumenthal, G., Faber, S., Primack, J. & Rees, M., 1984. *Nature*, **311**, 517.
Bond, J. R., Efstathiou, G., Lubin, P. M. & Meinhold, P. R., 1990. *Phys. Rev. Lett.*, submitted.

Börner, G. & Ehlers, J., 1988. *Astr. Astrophys.*, **204,** 1.

Boyle, B., 1991. In: *The Texas/ESO–CERN Symp.*, Brighton, UK, 1990, New York Academy of Sciences, New York, in press.

Coleman, S., 1988. *Nucl. Phys.*, **B307,** 643.

Davis, M., Efstathiou, G., Frenk, C. & White, S. D. M., 1985. *Astrophys. J.*, **292,** 371.

Dekel, A., Bertschinger, E. & Faber, S. M., 1990. *Astrophys. J.*, **364,** 349.

Efstathiou, G., Sutherland, W. J. & Maddox, S. J., 1990. *Nature*, **348,** 705.

Einstein, A., 1917. *Sitz. Preuss. Akad. d. Wiss.*, **1917**, 142 (English translation in: *The Principle of Relativity*, 1923, Dover, New York; reprinted in: *Cosmological Constants*, 1986, p. 16, eds Berstein, J. & Feinberg, G., Columbia Press, New York).

Evrard, A. E., 1989. *Astrophys. J. Lett.*, **341,** L71.

Felten, J. E. & Isaacman, R., 1986. *Rev. Mod. Phys.*, **58,** 689.

Fukugita, M. & Hogan, C., 1990. *Nature*, **347,** 120.

Fukugita, M., Takahara, F., Yamashita, K. & Yoshii, Y., 1990a. *Astrophys. J. Lett.*, **361,** L1.

Fukugita, M., Futamase, T. & Kasai, M., 1990b. *Mon. Not. R. astr. Soc.*, **246,** 24.

Gott, J. R., Park, M. G. & Lee, H. M., 1989. *Astrophys. J.*, **338,** 1.

Gramann, M., 1990. *Mon. Not. R. astr. Soc.*, **244,** 214.

Gunn, J. E., 1990. In: *Clusters of Galaxies*, eds Oegerle, W. R., Fitchett, M. J. & Danly, L., Cambridge University Press, Cambridge.

Gunn, J. E. & Gott, J. R., 1972. *Astrophys. J.*, **176,** 1.

Heath, D. J., 1977. *Mon. Not. R. astr. Soc.*, **179,** 351.

Holtzman, J., 1989. *Astrophys. J. Suppl.*, **71,** 1.

Jacobsen, P., Perryman, M. A. C., Ulrich, H. M., Machetto, F. & Di Serego Alighieri, S., 1986. *Astrophys. J. Lett.*, **303,** L27.

Kaiser, N., Efstathiou, G., Ellis, R., Frenk, C., Lawrence, A., Rowan-Robinson, M. & Saunders, W., 1991. *Mon. Not. R. astr. Soc.*, in press.

Kerszberg, P., 1989. *The Invented Universe*, Oxford University Press, New York.

Klebanov, I., 1990. In: *Actions to Answers: Proc. of TASI 1988*, eds T. DeGrand & D. Toussaint, World Scientific, Singapore.

Kofman, L. A. & Starobinsky, A. A., 1985. *Soviet Astr.*, **11,** 271.

Landau, L. D. & Lifshitz, E. M., 1960. *Mechanics*, Pergamon Press, Oxford.

Lightman, A. P. & Schechter, P. L., 1990. *Astrophys. J. Suppl.*, **74**.

Lilje, P. B. & Lahav, O., 1991. *Astrophys. J.*, in press (LL).

Linde, A., 1990. *Particle Physics and Inflationary Cosmology*, Gordon and Breach, New York.

Lynden-Bell, D., Lahav, O. & Burstein, D., 1989. *Mon. Not. R. astr. Soc.*, **241,** 325.

Martel, H., 1991a. *Astrophys. J.*, **366,** 353.

Martel, H., 1991b. *Astrophys. J.*, submitted.

Martel, H. & Wasserman, I., 1990. *Astrophys. J.*, **348,** 1.

Mellier, Y., Soucail, G., Fort, B., Mathez, G., 1988. *Astr. Astrophys.*, **199,** 13.

Olive, K. A., Schramm, D. N., Steigman, G. & Walker, T. P., 1990. *Phys. Lett.*, **236,** 454.

Peebles, P. J. E., 1980. *The Large Scale Structure of the Universe*, Princeton University Press, Princeton.

Peebles, P. J. E., 1984. *Astrophys. J.*, **284,** 439.

Peebles, P. J. E., 1988. *Publs. Astr. Soc. Pac.*, **100,** 670.

Petrosian, V., Salpeter, E. E. & Szekeres, P., 1967. *Astrophys. J.*, **147,** 1222.

Rabinovici, E., Saering, B. & Bardeen, W. A., 1987. *Phys. Rev. D.*, **36,** 562.

Regös, E. & Geller, M. J., 1989. *Astr. J.*, **98,** 755.

Rindler, W., 1977. *Essential Relativity*, Springer-Verlag, New York.

Rowan-Robinson, M., 1968. *Mon. Not. R. astr. Soc.*, **141,** 445.

Sandage, A. R. & Cacciari, C., 1990. *Astrophys. J.*, **350,** 645.

Schneider, D. P., Schmidt, M. & Gunn, J. E., 1989. *Astr. J.*, **98,** 1951.

Shklovsky, I., 1967. *Astrophys. J. Lett.*, **150,** L1.

Silk, J. & White, S. D. M., 1978. *Astrophys. J. Lett.*, **226,** L103.

Soucail, G., Mellier, Y., Fort, B., Hammer, F. & Mathez, G., 1987. *Astr. Astrophys.*, **184,** L7.

Stabell, R. & Refsdal, S., 1966. *Mon. Not. R. astr. Soc.*, **132,** 379.

Steinhardt, P. J., 1990. *Nature*, **345,** 47.

Strauss, M., 1989. *PhD thesis*, University of California, Berkeley.

Sugiyama, N., Gouda, N. & Sasaki, M., 1990. *Astrophys. J.*, **365,** 432.

Turner, E. L., 1990. *Astrophys. J. Lett.*, **365,** L43.

Turner, M. S., Steigman, G. & Krauss, L. M., 1984. *Phys. Rev. Lett.*, **52,** 2090.

Tyson, J. A., 1988. *Astr. J.*, **96,** 1.

Veneziano, G., 1989. *Mod. Phys. Lett.*, **A4,** 695.

Vittorio, N. & Silk, J., 1984. *Astrophys. J. Lett.*, **285,** L39.

Weinberg, S., 1987. *Phys. Rev. Lett.*, **59,** 2607.

Weinberg, S., 1989. *Rev. Mod. Phys.*, **61,** 1.

Yahil, A., 1985. In: *The Virgo Cluster of Galaxies*, p. 359, eds Richter, O. G. & Binggeli, B., ESO, Garching.

Yahil, A., 1990. In: *Proc. of the Moriond Conference*, March 1990.

Yahil, A., Strauss, M. A. & Davis, M., 1990. *Astrophys. J.*, submitted.